

Induction of functional hepatocyte-like cells from mouse fibroblasts by defined factors

Pengyu Huang¹, Zhiying He^{1,2}, Shuyi Ji¹, Huawang Sun¹, Dao Xiang², Changcheng Liu^{1,2}, Yiping Hu², Xin Wang^{1,3,4} & Lijian Hui¹

The generation of functional hepatocytes independent of donor liver organs is of great therapeutic interest with regard to regenerative medicine and possible cures for liver disease¹. Induced hepatic differentiation has been achieved previously using embryonic stem cells or induced pluripotent stem cells^{2–8}. Particularly, hepatocytes generated from a patient's own induced pluripotent stem cells could theoretically avoid immunological rejection. However, the induction of hepatocytes from induced pluripotent stem cells is a complicated process that would probably be replaced with the arrival of improved technology. Overexpression of lineage-specific transcription factors directly converts terminally differentiated cells into some other lineages^{9–12}, including neurons¹³, cardiomyocytes¹⁴ and blood progenitors¹⁵; however, it remains unclear whether these lineage-converted cells could repair damaged tissues *in vivo*. Here we demonstrate the direct induction of functional hepatocyte-like (iHep) cells from mouse tail-tip fibroblasts by transduction of Gata4, Hnf1 α and Foxa3, and inactivation of p19^{Arf}. iHep cells show typical epithelial morphology, express hepatic genes and acquire hepatocyte functions. Notably, transplanted iHep cells repopulate the livers of fumarylacetoacetate-hydrolase-deficient (*Fah*^{-/-}) mice and rescue almost half of recipients from death by restoring liver functions. Our study provides a novel strategy to generate functional hepatocyte-like cells for the purpose of liver engineering and regenerative medicine.

Fourteen mouse transcription factors (14TF, Supplementary Table 1) important for liver development and function^{16–19} were transduced into immortalized 3T3 fibroblasts, mouse embryonic fibroblasts (MEFs) and tail-tip fibroblasts (TTFs) via lentiviral infection. The hepatic genes albumin (*Alb*) and *Tdo2* were induced in these cells at day 5 after infection (Supplementary Fig. 1a), indicating that fibroblasts have the potential to be converted to hepatocytes. To ensure that the process is independent of spontaneous immortalization and embryonic progenitors, we focused on TTFs in the following study. Wild-type TTFs showed proliferation arrest and cell death within 7 days after transduction (Supplementary Fig. 1b), thereby inhibiting continuous hepatic conversion. Because p19^{Arf} (also called *Cdkn2a*)-null (p19^{Arf}^{-/-}) hepatocytes proliferate *in vitro* without losing genetic stability²⁰, we used p19^{Arf}^{-/-} TTFs to overcome the proliferative limitation (Fig. 1a). Remarkably, proliferative cells with epithelial morphology were induced from mesenchymal p19^{Arf}^{-/-} TTFs after transduction of 14TF (Supplementary Fig. 1b). Moreover, these cells expressed *Alb*, *Tdo2* and *Ttr* (Supplementary Fig. 1c).

Eleven epithelial colonies, picked up at day 21 after lentiviral transduction, expressed hepatic genes and the exogenous 14TF at different levels (Supplementary Fig. 2). One epithelial colony, ET26, was further characterized (Fig. 1b). ET26 cells expressed hepatic secretory protein genes, cytokeratin genes, epithelial cell adhesion genes and endogenous hepatic transcription factors (Fig. 1c). By contrast, expression of *Col1a1*, *Pdgfrb*, *Postn* and *Fsp1* (also called *S100a4*), genes typical for fibroblast, was downregulated in ET26 cells (Fig. 1c). Functionally, ET26 cells showed glycogen storage as demonstrated by periodic acid-Schiff

(PAS) staining (Fig. 1d) and uptake of DiI-labelled acetylated low-density lipoprotein (DiI-ac-LDL, Fig. 1e). These results indicated that p19^{Arf}^{-/-} TTFs were converted into cells with significant hepatic gene expression and hepatic functions.

Next, we determined the key factors required for hepatic conversion. On the basis of previous reports^{16–19}, we established combinations of six factors (6TF), including Foxa2, Foxa3, Hnf1 α , Hnf4 α , Hnf6 and Gata4, and eight factors (8TF), including 6TF plus Foxa1 and Hnf. Either 6TF or 8TF converted TTFs to epithelial colonies with hepatic gene expression at comparable levels (Supplementary Fig. 3a, b). Upon withdrawal of Hnf6 from 6TF, we found significantly increased

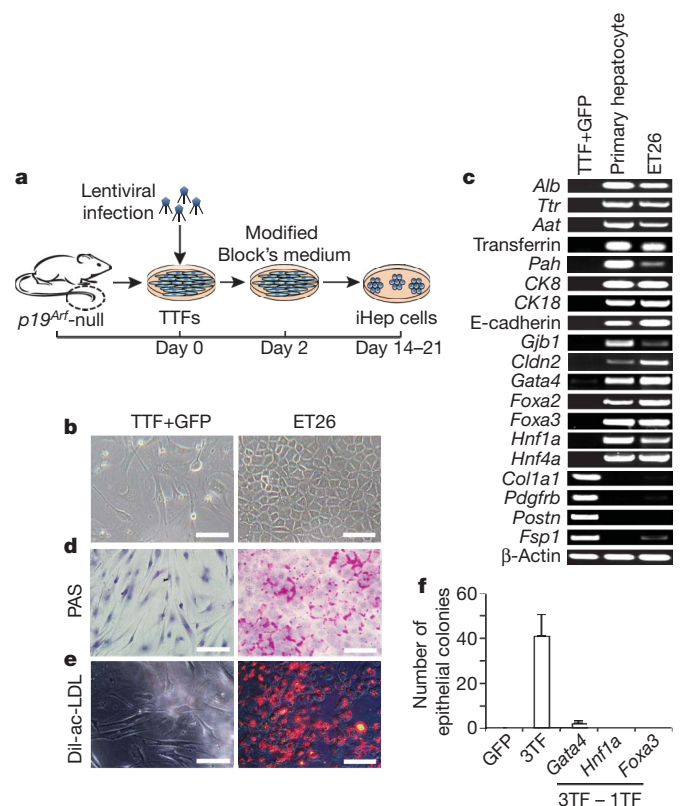


Figure 1 | Three transcription factors induce hepatic conversion of tail-tip fibroblasts. **a**, Experimental design of iHep cell induction. Primary p19^{Arf}^{-/-} TTFs were infected with lentiviruses expressing hepatic transcription factors. Cultures were changed to modified Block's medium 2 days after infection. **b**, Colony ET26 shows epithelial morphology. **c**, Expression of the indicated genes was measured by RT-PCR in ET26 cells, primary hepatocytes and TTFs. **d**, Cytoplasmic accumulation of glycogen was determined by PAS staining (purple cytoplasmic staining). **e**, Intake of DiI-ac-LDL in ET26 cells (red staining). All scale bars: 100 μ m. **f**, Effects of individual factor withdrawal from 3TF on epithelial colony formation. Data are presented as mean + s.d.

¹Laboratory of Molecular Cell Biology, Institute of Biochemistry and Cell Biology, Shanghai Institutes for Biological Sciences, Chinese Academy for Sciences, Yueyang Road 320, 200031 Shanghai, China. ²Department of Cell Biology, Second Military Medical University, 800 Xiangyin Road, 200433 Shanghai, China. ³Department of Laboratory Medicine and Pathology, University of Minnesota, Minneapolis, 55455 Minnesota, USA. ⁴Stem Cell Institute, University of Minnesota, Minneapolis, 55455 Minnesota, USA.

hepatic gene expression and epithelial colony formation (Supplementary Fig. 3a, b). For the remaining five factors (5TF), removal of *Hnf4 α* further promoted the formation of epithelial colonies (Supplementary Fig. 3c). The remaining four factors were further grouped into two combinations: *Gata4*, *Hnf1 α* and *Foxa3* (3TF) and *Gata4*, *Hnf1 α* and *Foxa2* (3TF'). 3TF showed a stronger effect than 3TF' on the induction of hepatic gene expression and epithelial colony formation (Supplementary Fig. 3d and data not shown). Remarkably, 3TF induced endogenous *Foxa2* and *Foxa3* expression (Supplementary Fig. 3d), and removal of any factor from 3TF failed to form epithelial colonies (Fig. 1f). Intriguingly, 3TF triggered *p19^{Arf}*^{-/-} MEFs to express hepatic genes (Supplementary Fig. 4), indicating the potential to induce hepatic conversion of embryonic fibroblasts. Upon RNA-interference-mediated knockdown of *p19^{Arf}*, 3TF also converted wild-type TTFs to epithelial cells with hepatic gene expression (Supplementary Fig. 5).

iHep cells induced by the overexpression of *Gata4*, *Hnf1 α* and *Foxa3* and the inactivation of *p19^{Arf}* were characterized for their hepatic features. At day 6, the epithelial cells induced by 3TF were positively stained for tight junction protein 1 (Tjp1) and E-cadherin (Fig. 2a–c). At day 14, 23% of epithelial cells were positive for Alb (Supplementary Fig. 6a), indicating an efficient hepatic conversion. The increased expression of hepatic genes over time, for example, *Alb*, *Ttr*, transferrin (*Ttrf*) and *CK18* (also called *Krt18*), showed a progressively enhanced reprogramming (Fig. 2d and Supplementary Fig. 6b, $P < 0.05$). Interestingly, iHep cells also expressed *Afp* and *CK19* (also called *Krt19*) (Fig. 2d). Protein expression of Alb and *Hnf4 α* was confirmed by immunofluorescent staining in iHep cells (Supplementary Fig. 6c, d). Notably, expression levels of exogenous 3TF were markedly decreased during hepatic conversion, indicating that continuous expression of exogenous 3TF is not required (Supplementary Fig. 6e).

Individual iHep colonies showed similar expression patterns of hepatic genes and fibrotic genes (Supplementary Fig. 6f), indicating

a homogeneous conversion among individual TTFs. Although iHep cells expressed *Afp* and *CK19* (Fig. 2d), other hepatoblast marker genes, such as *Lin28b*, *Igf2* and *Dlk1* (ref. 8), were undetectable during hepatic conversion (Supplementary Fig. 7a). Importantly, cytochrome P450 (CYP) enzymes specific to mature hepatocytes were detectable in iHep cells (Supplementary Fig. 7b), suggesting that hepatic conversion undertakes a process without reversion to progenitors. Moreover, iHep cells neither expressed bile duct marker genes nor formed branching bile duct tubes *in vitro* (Supplementary Fig. 7c, d). The marker genes for pancreatic exocrine and endocrine cells and intestinal cells were also undetectable (Supplementary Fig. 7e, f). Therefore, TTFs are not converted to lineages other than hepatocytes.

We compared the global expression profiles among iHep cells, TTFs, MEFs and hepatocytes cultured for 6 days. Pearson correlation analysis showed that iHep cells were clustered with cultured hepatocytes but separated from TTFs and MEFs (Fig. 2e). Microarray data revealed that numerous hepatic functional genes were upregulated in iHep cells compared to TTFs (Supplementary Figs 8 and 9). When compared with cultured hepatocytes, 877 out of 29,153 annotated genes were found to be upregulated in iHep cells, including *Afp*, *CK19*, *Fabp4* and *S100a9*, whereas 817 genes were downregulated, such as *Cyp4b1*, *Cyp2c40* and *Apob* (fold change > 2 , $P < 0.01$, *t*-test). Notably, iHep cells established substantial hepatic functions. iHep cells accumulated PAS-positive glycogen aggregations and transported DiI-ac-LDL into the cytoplasm (Fig. 2f, g). Indocyanine green uptake was found in 20% of iHep cells (Fig. 2h). Furthermore, iHep cells secreted high amounts of Alb into medium (Fig. 2i, $P < 0.05$). Importantly, iHep cells metabolized phenacetin, testosterone and diclofenac (Fig. 2j–l and Supplementary Fig. 10a–c, $P < 0.05$), whereas metabolic activity for bufuralol was undetected (Supplementary Fig. 10d).

Fah^{-/-} mice defective in tyrosine metabolism require 2-(2-nitro-4-trifluoro-methylbenzoyl)-1,3-cyclohexanedione (NTBC) supply for survival^{21–24}. After NTBC withdrawal (NTBC-off), *Fah*^{-/-} mice

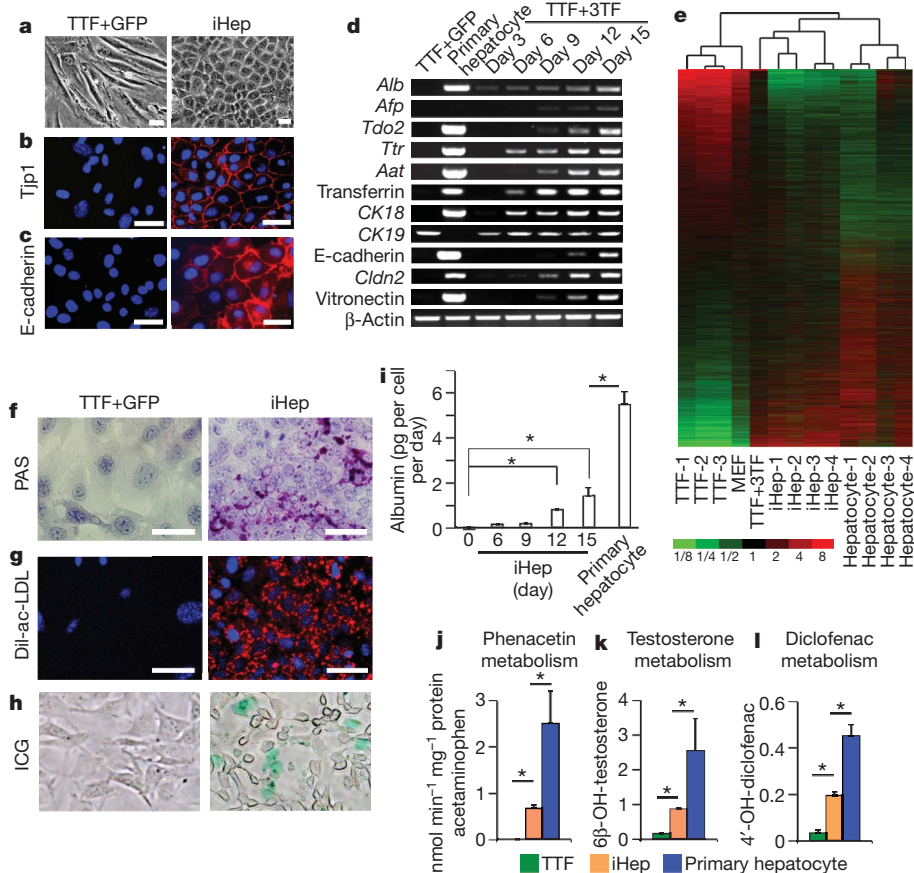


Figure 2 | Characterization of iHep cells *in vitro*.

a, 3TF-induced iHep cells show typical epithelial morphology. **b**, **c**, Epithelial conversion of TTFs was confirmed by immunofluorescent staining of Tjp1 and E-cadherin (red membrane staining). Nuclei are stained blue by DAPI. **d**, Expression of indicated genes was analysed by RT-PCR during the induction of iHep cells. **e**, Global gene expression by cDNA microarray assay. Expression profiles were clustered by a Pearson correlation analysis. Expression levels are depicted in colour. TTF+3TF, 3TF-transduced TTFs without enrichment of epithelial cells. Hepatocyte, hepatocytes cultured for 6 days. **f**, Glycogen storage was assayed by PAS staining. **g**, DiI-ac-LDL uptake in iHep cells. **h**, ICG uptake in iHep cells (green staining). **i**, Secretory albumin protein levels were measured by ELISA during hepatic conversion. **j–l**, CYP metabolic activities of iHep cells. The metabolic products of phenacetin (converted to acetaminophen by *Cyp1a2*; **j**), testosterone (converted to 6 β -OH-testosterone by *Cyp3a* enzymes; **k**) and diclofenac (converted to 4'-OH-diclofenac by *Cyp2c* enzymes; **l**) were determined by liquid chromatography-tandem mass spectrometry according to standard curve. *, $P < 0.05$, *t*-test. All scale bars: 50 μ m. Data are presented as mean \pm s.d. in **i–l**.

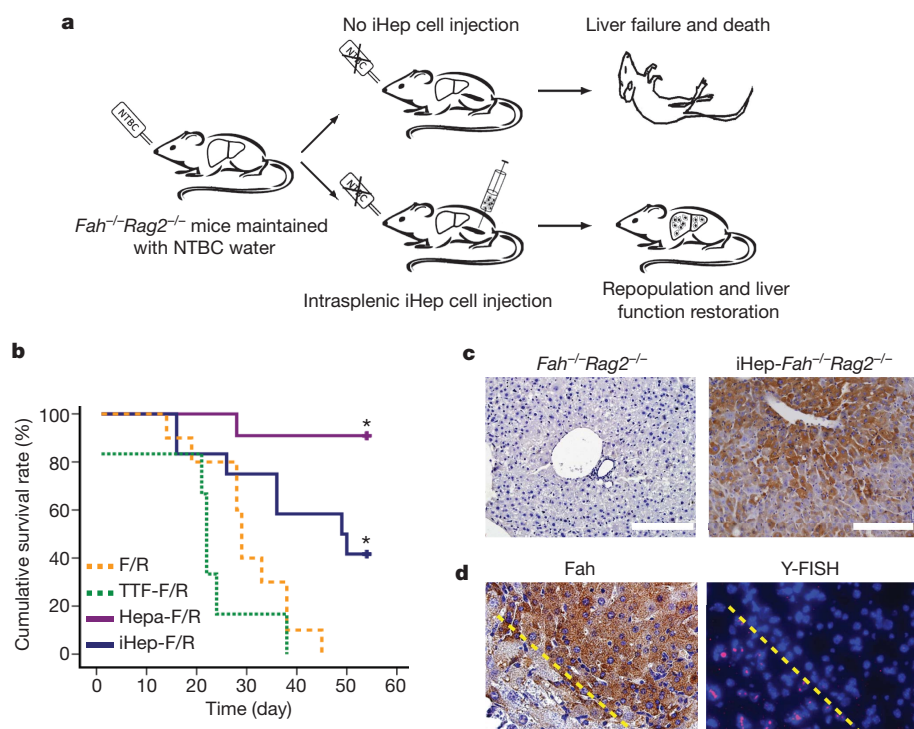


Figure 3 | iHep cell transplantation rescues Fah-deficient mice. **a**, Schematic outline of iHep cell transplantation into livers of $Fah^{-/-} Rag2^{-/-}$ mice.

b, Kaplan-Meier survival curve of primary-hepatocyte-transplanted $Fah^{-/-} Rag2^{-/-}$ mice (Hepa-F/R, $n = 10$), iHep-cell-transplanted $Fah^{-/-} Rag2^{-/-}$ mice (iHep-F/R, $n = 12$), TTF-transplanted $Fah^{-/-} Rag2^{-/-}$ mice (TTF-F/R, $n = 6$) and control $Fah^{-/-} Rag2^{-/-}$ mice (F/R, $n = 10$) after NTBC withdrawal. *, $P < 0.02$, log-rank test. **c**, Repopulation of iHep cells in $Fah^{-/-} Rag2^{-/-}$ livers was determined by Fah immunostaining (brown cytoplasmic staining).

d, Female iHep cells were transplanted into male $Fah^{-/-} Rag2^{-/-}$ livers. Serial liver sections were stained for both Fah immunostaining and Y-chromosome FISH staining (red dots). The boundary of the Fah^+ nodule is indicated by a dashed yellow line.

undergo liver failure and death. They can be rescued by transplantation of wild-type primary hepatocytes^{21–24}, representing a useful model to characterize *in vivo* repopulation and functions of iHep cells. Immunodeficient $Fah^{-/-} Rag2^{-/-}$ mice were used for transplantation to reduce the likelihood of immunological rejection (Fig. 3a, b and Supplementary Fig. 11a). Ten $Fah^{-/-} Rag2^{-/-}$ mice without transplantation were all dead within 6.5 weeks after NTBC-off and showed continuous loss of body weight (Fig. 3b and Supplementary Fig. 11b). Six $Fah^{-/-} Rag2^{-/-}$ mice transplanted with $p19^{Acf-/-}$ TTFs were also dead after NTBC-off (Fig. 3b). In contrast, 5 out of 12 $Fah^{-/-} Rag2^{-/-}$ mice transplanted with iHep cells (iHep- $Fah^{-/-} Rag2^{-/-}$) were alive 8 weeks after NTBC-off and showed increased body weight (Fig. 3b and Supplementary Fig. 11b, $P < 0.05$). Fah-positive (Fah^+) iHep cells engrafting into liver sinusoid comprised between 5% to 80% of total hepatocytes in iHep- $Fah^{-/-} Rag2^{-/-}$ livers (Fig. 3c and Supplementary Fig. 11c). Moreover, *Fah*-wild-type and $p19^{Acf}$ -null alleles were detected in iHep- $Fah^{-/-} Rag2^{-/-}$ livers by genomic PCR (Supplementary Fig. 11d). To exclude the possibility of cell fusion between iHep and host

cells, we stained the Y chromosome in male livers transplanted with female iHep cells. Twenty-five Fah^+ nodules in four male recipients were characterized and were all negative for Y-chromosome staining, confirming that iHep cells do not fuse with host cells (Fig. 3d and Supplementary Fig. 11e). These results indicate that transplanted iHep cells can repopulate and rescue $Fah^{-/-} Rag2^{-/-}$ recipients.

Macroscopically, iHep- $Fah^{-/-} Rag2^{-/-}$ livers are normal and healthy, whereas livers from NTBC-off $Fah^{-/-} Rag2^{-/-}$ control mice were swelled with many necrotic lesions (Fig. 4a). The hexagonal hepatic lobule was destructured due to massive cell death in NTBC-off $Fah^{-/-} Rag2^{-/-}$ livers (Supplementary Fig. 12a). In contrast, iHep cell repopulation restored liver architecture without apparent cell death (Supplementary Fig. 12a, b). Remarkably, both repopulated iHep cells and repopulated primary hepatocytes expressed Alb and other hepatic genes at comparable levels in $Fah^{-/-} Rag2^{-/-}$ recipient mice (Supplementary Fig. 12c, d). Moreover, serum levels of tyrosine, phenylalanine, ornithine, alanine and glycine were markedly reduced in iHep- $Fah^{-/-} Rag2^{-/-}$ mice compared to NTBC-off $Fah^{-/-} Rag2^{-/-}$

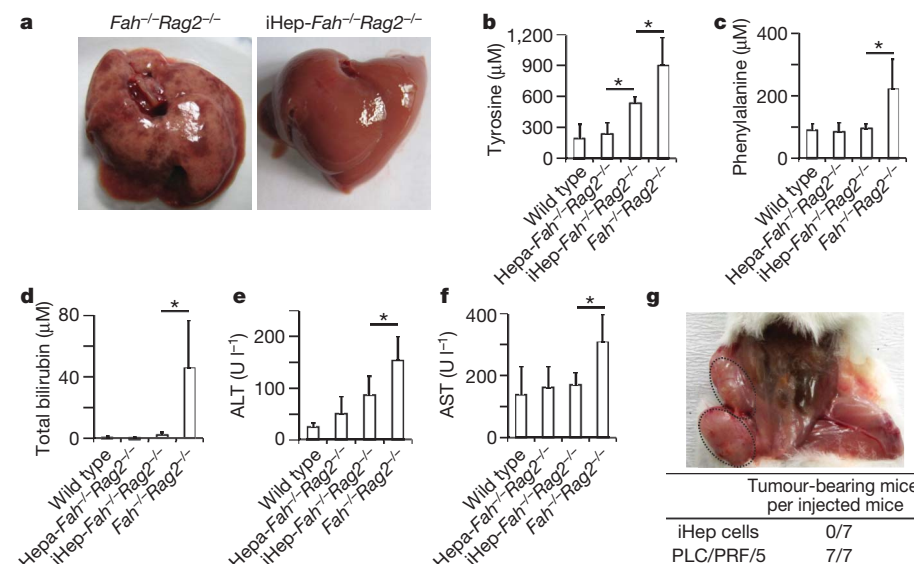


Figure 4 | iHep cells restore liver functions of $Fah^{-/-} Rag2^{-/-}$ mice. **a**, Representative pictures of whole livers from $Fah^{-/-} Rag2^{-/-}$ and iHep- $Fah^{-/-} Rag2^{-/-}$ mice. **b–f**, Serum levels of tyrosine (**b**), phenylalanine (**c**), total bilirubin (**d**), ALT (**e**) and AST (**f**) in wild-type ($n = 6$), Hepa- $Fah^{-/-} Rag2^{-/-}$ ($n = 5$), iHep- $Fah^{-/-} Rag2^{-/-}$ ($n = 5$, sera collected 8 weeks after iHep transplantation) and control $Fah^{-/-} Rag2^{-/-}$ mice ($n = 4$, sera collected upon losing 20% of body weight). *, $P < 0.05$, *t*-test. Data are presented as mean \pm s.d. **g**, iHep and PLC/PRF/5 cells (human hepatoma cell line) were subcutaneously transplanted into the left and right flanks of NOD/SCID mice, respectively. PLC/PRF/5-generated tumours are indicated by the dotted ovals.

mice (Fig. 4b, c, Supplementary Fig. 12e–g, and Supplementary Table 2, $P < 0.05$). iHep-*Fah*^{-/-}*Rag2*^{-/-} mice also showed decreased levels of total bilirubin, alanine aminotransferase (ALT) and aspartate aminotransferase (AST) (Fig. 4d–f and Supplementary Table 3, $P < 0.05$). These data demonstrate that iHep cell transplantation substantially improves liver functions of NTBC-off *Fah*^{-/-}*Rag2*^{-/-} mice.

Tumours were not found in iHep-*Fah*^{-/-}*Rag2*^{-/-} livers 2 months after transplantation. Ki67 staining revealed that iHep cells ceased proliferation 8 weeks after transplantation (Supplementary Fig. 13a). Moreover, iHep cells did not form tumours 8 weeks after subcutaneous xenograft in NOD/SCID mice (Fig. 4g). A total of 20 out of 25 analysed iHep cells displayed 40 chromosomes after 17 passages (Supplementary Fig. 13b), which was comparable with results from wild-type cells (data not shown). These results indicate that iHep cells do not seem to be tumour prone.

To our knowledge, this is the first time that adult fibroblasts have been directly converted to functional iHep cells. Together with previous findings^{9–15}, our results prove the general principle that cell lineages can be converted by regulating the transcriptional network. We identified the combination of Gata4, Foxa3 and Hnf1 α as being sufficient to induce hepatic conversion. Gata4 and Foxa3 probably act as ‘pioneer factors’ to trigger a global chromatin modification during hepatic conversion^{25,26}. Hnf1 α probably stabilizes the hepatic gene expression, as Hnf1 α , Foxa2 and Hnf4 α occupy each other’s promoters and maintain the hepatic phenotype^{16,27}. Moreover, we obtained proliferative iHep cells under the condition of inactivating p19^{Arf}. Because p19^{Arf} is a key component of the cellular senescence pathway that inhibits induced pluripotent stem cell reprogramming²⁸, it would be of interest to characterize whether inactivating other components of this pathway, such as p38 α ²⁹, could be used to facilitate hepatic conversion.

iHep cells showed an expression profile and hepatic function close to those of mature hepatocytes. Interestingly, some CYP genes were not induced in iHep cells, and *CK19* and *Afp* were upregulated. Moreover, iHep cell transplantation showed that the rescue was partial, suggesting that iHep cells are not identical to hepatocytes. Nevertheless, in contrast with any other cell-type conversion via lineage-specific transcription factors^{13–15}, the *in vivo* function of iHep cells has been rigorously proven. More importantly, iHep cells do not seem to be prone to tumour formation. Thus, iHep cells represent an alternative source of hepatocytes for disease modelling, transplantation and tissue engineering. To apply this approach for the purpose of regenerative medicine, future studies will need to address whether human fibroblasts and other cell types could be successfully converted to functional iHep cells.

METHODS SUMMARY

p19^{Arf}^{-/-}, *Fah*^{-/-}*Rag2*^{-/-} and NOD/SCID mice were maintained according to institutional regulation. *p19*^{Arf}^{-/-} TTFs between passage 7 and 9 were used for induction of iHep cells. *p19*^{Arf}^{-/-} TTFs were seeded on collagen-I-coated dishes and infected with lentiviruses expressing transcription factors. Cells were then cultured in Block’s medium containing 0.1 μ M dexamethasone, 20 μ g l⁻¹ TGF- α , 10 μ g l⁻¹ EGF, 4.2 mg l⁻¹ insulin, 3.8 mg l⁻¹ human transferrin, and 5 μ g l⁻¹ sodium selenite. Fourteen days after infection, we treated cells with 0.01% trypsin and discarded detached fibroblastic cells to enrich the epithelial cells. iHep cells were transplanted into spleens of *Fah*^{-/-}*Rag2*^{-/-} mice at the age of 8–12 weeks. We intrasplenically injected 8.33×10^5 iHep cells into *Fah*^{-/-}*Rag2*^{-/-} mice. NTBC was withdrawn from the drinking water after transplantation. Surviving *Fah*^{-/-}*Rag2*^{-/-} mice transplanted with iHep cells were killed 8 weeks after the surgery to collect peripheral blood and liver samples. All animal experiments were performed according to institutional regulations. Microarray data have been deposited in the Gene Expression Omnibus database (GSE23635).

Full Methods and any associated references are available in the online version of the paper at www.nature.com/nature.

Received 23 August 2010; accepted 15 April 2011.

Published online 11 May 2011.

- Zern, M. A. Cell transplantation to replace whole liver transplantation. *Gastroenterology* **136**, 767–769 (2009).
- Gouon-Evans, V. et al. BMP-4 is required for hepatic specification of mouse embryonic stem cell-derived definitive endoderm. *Nature Biotechnol.* **24**, 1402–1411 (2006).

- Soto-Gutiérrez, A. et al. Reversal of mouse hepatic failure using an implanted liver-assist device containing ES cell-derived hepatocytes. *Nature Biotechnol.* **24**, 1412–1419 (2006).
- Duan, Y. et al. Differentiation and enrichment of hepatocyte-like cells from human embryonic stem cells *in vitro* and *in vivo*. *Stem Cells* **25**, 3058–3068 (2007).
- Basma, H. et al. Differentiation and transplantation of human embryonic stem cell-derived hepatocytes. *Gastroenterology* **136**, 990–999 (2009).
- Si-Tayeb, K. et al. Highly efficient generation of human hepatocyte-like cells from induced pluripotent stem cells. *Hepatology* **51**, 297–305 (2010).
- Sullivan, G. J. et al. Generation of functional human hepatic endoderm from human induced pluripotent stem cells. *Hepatology* **51**, 329–335 (2010).
- Li, F. et al. Hepatoblast-like progenitor cells derived from embryonic stem cells can repopulate livers of mice. *Gastroenterology* **139**, 2158–2169 (2010).
- Shen, C. N., Slack, J. M. & Tosh, D. Molecular basis of transdifferentiation of pancreas to liver. *Nature Cell Biol.* **2**, 879–887 (2000).
- Xie, H., Ye, M., Feng, R. & Graf, T. Stepwise reprogramming of B cells into macrophages. *Cell* **117**, 663–676 (2004).
- Zhou, Q., Brown, J., Kanarek, A., Rajagopal, J. & Melton, D. A. *In vivo* reprogramming of adult pancreatic exocrine cells to β -cells. *Nature* **455**, 627–632 (2008).
- Feng, R. et al. PU.1 and C/EBP α / β convert fibroblasts into macrophage-like cells. *Proc. Natl Acad. Sci. USA* **105**, 6057–6062 (2008).
- Vierbuchen, T. et al. Direct conversion of fibroblasts to functional neurons by defined factors. *Nature* **463**, 1035–1041 (2010).
- Ieda, M. et al. Direct reprogramming of fibroblasts into functional cardiomyocytes by defined factors. *Cell* **142**, 375–386 (2010).
- Szabo, E. et al. Direct conversion of human fibroblasts to multilineage blood progenitors. *Nature* **468**, 521–526 (2010).
- Kyrmizi, I. et al. Plasticity and expanding complexity of the hepatic transcription factor network during liver development. *Genes Dev.* **20**, 2293–2305 (2006).
- Zaret, K. S. Genetic programming of liver and pancreas progenitors: lessons for stem-cell differentiation. *Nature Rev. Genet.* **9**, 329–340 (2008).
- Schrem, H., Klempnauer, J. & Borlak, J. Liver-enriched transcription factors in liver function and development. Part I: the hepatocyte nuclear factor network and liver-specific gene expression. *Pharmacol. Rev.* **54**, 129–158 (2002).
- Schrem, H., Klempnauer, J. & Borlak, J. Liver-enriched transcription factors in liver function and development. Part II: the C/EBPs and D site-binding protein in cell cycle control, carcinogenesis, circadian gene regulation, liver regeneration, apoptosis, and liver-specific gene regulation. *Pharmacol. Rev.* **56**, 291–330 (2004).
- Mikula, M. et al. Immortalized p19ARF null hepatocytes restore liver injury and generate hepatic progenitors after transplantation. *Hepatology* **39**, 628–634 (2004).
- Grompe, M. et al. Loss of fumarylacetoacetate hydrolase is responsible for the neonatal hepatic dysfunction phenotype of lethal albino mice. *Genes Dev.* **7** (12A), 2298–2307 (1993).
- Wang, X. et al. The origin and liver repopulating capacity of murine oval cells. *Proc. Natl Acad. Sci. USA* **100** (Suppl. 1), 11881–11888 (2003).
- Grompe, M. et al. Pharmacological correction of neonatal lethal hepatic dysfunction in a murine model of hereditary tyrosinaemia type I. *Nature Genet.* **10**, 453–460 (1995).
- Overturf, K. et al. Hepatocytes corrected by gene therapy are selected *in vivo* in a murine model of hereditary tyrosinaemia type I. *Nature Genet.* **12**, 266–273 (1996).
- Zaret, K. S. et al. Pioneer factors, genetic competence, and inductive signaling: programming liver and pancreas progenitors from the endoderm. *Cold Spring Harb. Symp. Quant. Biol.* **73**, 119–126 (2008).
- Cirillo, L. A. et al. Opening of compacted chromatin by early developmental transcription factors HNF3 (FoxA) and GATA-4. *Mol. Cell* **9**, 279–289 (2002).
- Odum, D. T. et al. Control of pancreas and liver gene expression by HNF transcription factors. *Science* **303**, 1378–1381 (2004).
- Li, H. et al. The *Ink4/Arf* locus is a barrier for iPS cell reprogramming. *Nature* **460**, 1136–1139 (2009).
- Hui, L. et al. p38 α suppresses normal and cancer cell proliferation by antagonizing the JNK-c-Jun pathway. *Nature Genet.* **39**, 741–749 (2007).

Supplementary Information is linked to the online version of the paper at www.nature.com/nature.

Acknowledgements We would like to thank X. Chen, J. Cen, L. Zhang and J. Yuan for technical support, and F. Tang and D. Li for comments. The laboratory of L.H. is funded by the National Science Foundation of China (91019014) and the Chinese Academy of Sciences (KSCX2-YW-R-241, XDA01010402 and the Hundred Talents Program). The laboratory of X.W. is supported by the National Science Foundation of China (30801115), Chinese National 863 Plan Project (2006AA02Z474) and National Key Basic Research and Development Program of China (2007CB947102 and 2009CB941100).

Author Contributions L.H. conceived the project. P.H. performed most of the experiments. S.J. analysed the *in vitro* functions of iHep cells. H.S. analysed gene expression of iHep cells. L.H., X.W., P.H. and Z.H. designed the experiments for characterizing *in vivo* functions of iHep cells. P.H., Z.H., D.X., C.L. and Y.H. performed the *in vivo* experiments. L.H. and P.H. analysed the data. L.H., P.H. and X.W. wrote the manuscript.

Author Information Microarray data have been deposited in the Gene Expression Omnibus database under accession number GSE23635. Reprints and permissions information is available at www.nature.com/reprints. The authors declare no competing financial interests. Readers are welcome to comment on the online version of this article at www.nature.com/nature. Correspondence and requests for materials should be addressed to L.H. (ljhui@sibs.ac.cn).

METHODS

Mice. $p19^{Axf-/-}$ mice, $Fah^{-/-}Rag2^{-/-}$ mice and NOD/SCID mice were maintained in specific pathogen-free husbandry. $Fah^{-/-}Rag2^{-/-}$ mice were fed with drinking water containing 7.5 mg l^{-1} NTBC. The genetic background for $p19^{Axf-/-}$ and $Fah^{-/-}Rag2^{-/-}$ mice was C57Bl6/J \times 129Sv. $Fah^{-/-}Rag2^{-/-}$ mice were used as the recipient to reduce immunological rejection of iHep cells after transplantation.

Molecular cloning and lentivirus production. A multi-cloning site (CGGGA TCCCGCGCGCCGACTAGTCGACGCGTCGAGGTAACCTACGGACCGGT TT) was inserted into the PmeI restriction site of lentiviral vector pWPI (obtained from Addgene). cDNAs of candidate genes were cloned into the modified pWPI plasmid. For $p19^{Axf}$ shRNA expression, DNA oligonucleotides encoding $p19^{Axf}$ shRNA (CCGGGTGAACATGTTGTTGAGGCTAGGATCCTAGCCTCAACA ACATGTTCACTTTTGG) were inserted into the AgeI and EcoRI restriction sites of the pLKO.1 plasmid. Constructed pWPI or pLKO.1 plasmids were then introduced to 293FT cells together with packaging plasmid psPAX2 (Addgene) and envelope plasmid pMD2.G (Addgene). After 48 h incubation, the medium containing lentiviruses was collected and passed through a $0.45\ \mu\text{m}$ filter.

Fibroblast culture and bile duct induction. To isolate tail-tip fibroblasts, 5 cm of tail were cut from two-month-old mice. We peeled the dermis and minced tails into 1-cm pieces. Two pieces were placed per 60-mm collagen-I-coated dish in 5 ml DMEM (Sigma-Aldrich) containing 10% FBS (Sigma-Aldrich). After 5 days incubation, fibroblasts that migrated out of the tails were transferred to new collagen-I-coated dishes. We used TTFs between passage 7 and 9 for iHep cell induction. Embryonic fibroblasts were isolated from E13.5 embryos. Head and visceral tissue were dissected and removed. The remaining tissues were minced and incubated with 0.25% trypsin (Gibco) at 37°C for 15 min. Isolated cells were plated onto a 60-mm collagen-I-coated dish in 5 ml DMEM containing 10% FBS. We used MEFs at passage 3 for lentiviral infection.

For bile duct differentiation, 1×10^4 cells were re-suspended in 1 ml DMEM/F12 medium with 1 ml freshly prepared collagen gel solution and poured into a 35-mm dish. After gel solidification, cells were cultured with 1.5 ml DMEM/F12 supplemented with 10% FBS, $1 \times \text{ITS}$, $20\ \text{ng ml}^{-1}$ HGF for 3 days.

Primary hepatocyte isolation and culture. Adult mice were subjected to standard two-step collagenase perfusion for isolation of primary hepatocytes. Briefly, the liver was pre-perfused through the portal vein with calcium-free buffer ($0.5\ \text{mM}$ EGTA, $1 \times \text{EBSS}$ without Ca^{2+} and Mg^{2+}) and then perfused with collagenase ($0.2\ \text{mg ml}^{-1}$ collagenase type IV (Sigma), $10\ \text{mM}$ HEPES, $1 \times \text{EBSS}$ with Ca^{2+} and Mg^{2+}). Parenchymal cells were purified by Percoll buffer (90% Percoll (Sigma), $1 \times \text{EBSS}$) at low-speed centrifugation ($1,500\ \text{r.p.m.}$, 10 min). Viability of isolated hepatocytes was around 90% as determined by Trypan blue. For microarray analysis, $p19^{Axf-/-}$ primary hepatocytes were cultured in modified Block's medium supplemented with $0.1\ \mu\text{M}$ dexamethasone, $20\ \mu\text{g l}^{-1}$ TGF- α , $10\ \mu\text{g l}^{-1}$ EGF, $4.2\ \text{mg l}^{-1}$ insulin, $3.8\ \text{mg l}^{-1}$ human transferrin and $5\ \mu\text{g l}^{-1}$ sodium selenite in collagen-I-coated dishes for 6 days before harvesting for RNA extraction. For other experiments, $p19^{Axf-/-}$ primary hepatocytes were immediately lysated in Trizol for total RNA isolation.

PCR. For most experiments, total RNA was isolated from cells by Trizol (Invitrogen). For RNA extraction from formalin-fixed-paraffin-embedded (FFPE) tissues, four serial sections mounted on polyethylene terephthalate (PET) membrane frame slides were deparaffinized and air dried. The first section was stained with anti-Fah antibody to identify the repopulated Fah^+ nodules. On the basis of the result of Fah immunostaining in the first section, Fah^+ tissues within the nodules were microdissected from the following three sections by a Leica LMD7000 Laser Microdissection Microscope (Leica Microsystems) with laser intensity of 45 and speed of 5. After microdissection, the remaining sections on the slides were further stained with anti-Fah antibody to confirm that only tissues inside Fah^+ nodules were separated. Microdissected tissues from the same Fah^+ nodule were pooled together for total RNA extraction using RNeasy FFPE Kit (Qiagen).

A total of $1\ \mu\text{g}$ RNA was reverse transcribed into cDNA with M-MLV Reverse Transcriptase (Promega) according to the manufacturer's instructions. For DNA extraction from formalin-fixed-paraffin-embedded tissues, the QIAamp DNA FFPE Tissue Kit (Qiagen) was applied according to the manufacturer's instructions. PCR was performed with HiFi Taq polymerase (TransGen). Quantitative real-time PCR was performed with SYBR Premix Ex Taq (TaKaRa) on an ABI 7500 fast real-time PCR system (Applied Biosystems). Primer sequences will be provided upon request.

Immunofluorescence. For immunofluorescence staining, the cells were fixed with 4% paraformaldehyde for 15 min at room temperature, and then incubated with PBS containing 0.2% Triton X-100 (Sigma) for 15 min. Cells were then washed three times with PBS. After being blocked by 3% BSA in PBS for 60 min at room temperature, cells were incubated with primary antibodies at 4°C

overnight, washed three times with PBS, and then incubated with appropriate fluorescence-conjugated secondary antibody for 60 min at room temperature in the dark. Nuclei were stained with DAPI (Sigma). Primary and secondary antibodies were diluted in PBS containing 3% BSA. Antibodies used for immunofluorescence are as follows: mouse anti-Tjp1 (Invitrogen, 1:750), rabbit anti-E-cadherin (Cell Signaling, 1:500), mouse anti-albumin (R&D, 1:200), goat anti-Hnf4 α (Santa Cruz, 1:200). Cy5-conjugated goat anti-mouse IgG (Jackson Laboratories, 1:1,000), Cy3-conjugated goat anti-rabbit IgG (Jackson Laboratories, 1:1,000), Cy3-conjugated donkey anti-goat IgG (Jackson Lab, 1:1,000). For Y-chromosome fluorescent *in situ* hybridization (FISH), liver samples of male $Fah^{-/-}Rag2^{-/-}$ mice transplanted with female iHep cells were embedded in paraffin and hybridized with mouse Y-chromosome probe (ID Labs Inc., Canada) according to the manufacturer's instruction.

FACS analyses. For intracellular staining of albumin, 10^6 cells were harvested and fixed with 4% PFA for 30 min, and then permeabilized in staining buffer (PBS with 10% FBS and 0.5% saponin) for 10 min. Cells were then incubated with primary antibody (anti-albumin, R&D) for 30 min in staining buffer, followed with secondary antibody (Cy5-conjugated goat anti-mouse IgG, Jackson Laboratories) incubation for 30 min. Cells were analysed by the Calibur flow cytometer (Becton Dickinson). Data were analysed with Windows Multiple Document Interface for Flow Cytometry (WinMDI, version 2.9).

PAS stain, DiI-ac-LDL and ICG uptake assays, Alb ELISA and CYP metabolism assay. Cells were stained by periodic acid-Schiff (PAS, Sigma) and DiI-ac-LDL (Invitrogen) following the manufacturer's instructions. For the indocyanine green (ICG, Sigma) uptake assay, cells were cultured in the medium supplemented with progesterone, pregnenolone-16 α -carbonitrile and 8-bromo cAMP for 2 days. Cells had their medium changed with $1\ \text{mg ml}^{-1}$ ICG and were incubated at 37°C for 1 h, followed by washing with PBS three times.

To determine Alb secretion, TTFs transduced with three factors were cultured in the medium without phenol red. Culture supernatant was collected 24 h after medium change. The amount of Alb in the supernatant was determined by the mouse albumin ELISA kit (Bethyl Laboratory) according to the manufacturer's instructions.

For the measurement of CYP enzyme activities, TTFs and iHep cells were cultured in the medium with $50\ \mu\text{M}$ 3-methylcholanthrene for 48 h. Cells were dissociated and incubated with substrate in $200\ \mu\text{l}$ incubation medium at different concentrations for 3 h at 37°C . To stop the reaction, $800\ \mu\text{l}$ cold methanol was added and centrifuged. The supernatants were collected for measurement of indicated productions by LC-MS/MS (Agilent 1200 HPLC and ABI 4000 mass spectrometer). Freshly isolated hepatocytes were used as a positive control. Total cell protein amount was used to normalize the data. Substrates and metabolic products for standard were commercially purchased: phenacetin, diclofenac, bufuralol, acetaminophen, 4'-OH diclofenac (Sigma), testosterone (Fluka), 6 β -OH-testosterone (Cerilliant) and 1'-OH-bufuralol (Toronto Research Chemicals).

Microarray analysis. Total RNA extracted from $p19^{Axf-/-}$ TTFs, $p19^{Axf-/-}$ MEFs, $p19^{Axf-/-}$ hepatocytes cultured for 6 days, 3TF-transduced $p19^{Axf-/-}$ TTFs without enrichment of epithelial cells, and iHep cells from different experiments was hybridized to whole mouse gene expression microarray (Agilent) under the manufacturer's instruction. Data were normalized by Gene-Spring (Agilent). Microarray hybridization and analysis were carried out by ShanghaiBio Cooperation. Out of 29,153 annotated genes, 11,797 genes for which expression levels were at least twofold different between $p19^{Axf-/-}$ TTFs and primary $p19^{Axf-/-}$ hepatocytes were selected for analyses. Hierarchical clustering of samples was performed by Cluster 3.0 software. Average linkage with the uncentred correlation similarity metric was used for the clustering of samples. Original data were uploaded to the Gene Expression Omnibus database (accession number GSE23635).

In vivo function analysis. $Fah^{-/-}Rag2^{-/-}$ mice were maintained with $7.5\ \text{mg l}^{-1}$ NTBC in the drinking water. According to our previous experience with primary hepatocyte and ES-cell-derived hepatoblast transplantation, 8.33×10^5 iHep cells and 8.33×10^5 $p19^{Axf-/-}$ TTFs were transplanted into the spleens of $Fah^{-/-}Rag2^{-/-}$ mice at the age of 8–12 weeks, respectively. NTBC was withdrawn from the drinking water after cell transplantation. Ten $Fah^{-/-}Rag2^{-/-}$ mice without any transplantation also had NTBC withdrawn as a control. A survival curve was generated by SPSS for windows using Kaplan–Meier method. Eight weeks after transplantation, the blood of surviving iHep-cell-transplanted $Fah^{-/-}Rag2^{-/-}$ mice was collected from the retro-orbital sinus and centrifuged at $12,000\ \text{r.p.m.}$ for 15 min. The serum was frozen at -80°C until biochemical analyses. Total bilirubin, albumin, ALT, AST, blood urea nitrogen and creatinine were measured by 7600-020 clinical analyser (Hitachi). Amino acids were quantified by liquid chromatography-mass spectrometry ABI 3200 Q TRAP LC-MS/MS system (Applied Biosystem). After blood collection, mice were killed by cervical dislocation and livers were harvested, fixed and stained with Fah polyclonal antibody or haematoxylin and eosin as previously described. Blood and liver samples of control NTBC-off $Fah^{-/-}Rag2^{-/-}$ mice were collected after losing 20% body weight.

Tumour generation assay. The human hepatoma cell line PLC/PRF/5 was cultured in the same medium as iHep cells. iHep cells were induced and enriched as described above. After 21 days induction, cells were detached by trypsin and suspended in PBS. Seven NOD/SCID mice respectively were injected with 5×10^6 iHep cells in the left subcutaneous flank and 5×10^6 PLC/PRF/5 cells in the right subcutaneous flank. Tumour numbers were counted 8 weeks after injection.

Statistics. All data are presented as mean + s.d. For most statistical evaluation, an unpaired Student's *t*-test was applied for calculating statistical probability in this study. For survival analysis, the Mantel–Cox log-rank test was applied. Statistical calculation was performed using Statistical Program for Social Sciences software (SPSS, IBM). For all statistics, data from at least three independent samples or repeated experiments were used.